Concentrated Aqueous Micellar Solutions of Diblock Copoly(oxyethylene/oxybutylene) $E_{41}B_8$: A Study of Phase Behavior

Hong Li, Ga-Er Yu, Colin Price, and Colin Booth*

Manchester Polymer Centre, Department of Chemistry, University of Manchester, Manchester M13 9PL, U.K.

Edgar Hecht and Heinz Hoffmann

Physical Chemistry 1, University of Bayreuth, D-95440 Bayreuth, Germany

Received October 15, 1996; Revised Manuscript Received January 2, 1997[⊗]

ABSTRACT: A phase diagram is presented for aqueous solutions of oxyethylene/oxypropylene (E/B) block copolymer $E_{41}B_8$. The concentration range covered is 5−70 wt %. The range of techniques used (tube inversion, polarized-light microscopy, rheometry, and differential scanning calorimetry) enabled regions to be assigned to micellar sol, isotropic soft gel, isotropic cubic gel, and birefringent hexagonal gel. The soft gel is assigned to a fractal network formed from spherical micelles and highly swollen by the water phase.

1. Introduction

Block copolymers of ethylene oxide and 1,2-butylene oxide (systematic name 1,2-epoxybutane) in aqueous solution self-associate to form spherical micelles at low concentration. We denote diblock copolymers E_mB_n, where E = the oxyethylene unit [OCH_2CH_2] and B = the oxybutylene unit [$OCH_2CH(C_2H_5)$], with corresponding nomenclature for other architectures (e.g. $E_mB_nE_m$). A limited range of oxyethylene/oxybutylene block copolymers is available from the Dow Chemical Co.,[1,2] but those described in the present report were synthesized in Manchester.

Because of the hydrophobicity of the B unit, the critical micelle concentrations (cmc) of these copolymers can be very low:[3,4] e.g. copolymer $E_{24}B_{10}$ at 40 °C, cmc ≈ 0.002 wt %, and copolymer $E_{45}B_{15}E_{45}$ at 37 °C, cmc ≈ 0.013 wt %. Micelles and molecules are in dynamic equilibrium at all temperatures and concentrations above the critical condition, but the proportion of molecules becomes progressively smaller as temperature and/or concentration is increased. At moderately high concentrations the micelles may pack to form stiff gels. Typically, on heating a solution of concentration 25 wt % the system will undergo the transitions sol → gel → sol. In our previous work a tube-inversion method was used to define the transition temperatures, a method which is sensitive to the yield stress of the gel. The first such phase diagram reported[5] for an E/B copolymer ($E_{58}B_{17}E_{58}$) is shown in Figure 1. Under the polarized-light microscope such gel phases are found to be isotropic and can be characterized as cubic liquid-crystal phases formed by packing spherical micelles of much the same size as those in dilute micellar solution.[6] The transitions between gel and sol are very sharp, covering no more than a fraction of a degree.

Similar gels are formed by some of the familiar $E_mP_nE_m$ triblock copolymers (P represents an oxypropylene unit [$OCH_2CH(CH_3)$]), known commercially by their trade names, e.g. Pluronic (BASF Corp.) or Synperonic PE (ICI Plc) polyols. Gelation of solutions of these copolymers, including low- and high-temperature transitions, was recognized many years ago,[7] but phase diagrams similar to that in Figure 1 were not published until 1992.[8−10] Recently aqueous $E_mP_nE_m$ copolymer solutions have been extensively studied in a number of laboratories, providing evidence of cubic, hexagonal, and lamella liquid-crystalline phases. Recent publications include many relevant references.[11−13] Under certain conditions, a bicontinuous sponge-like L_3 phase is formed.[12]

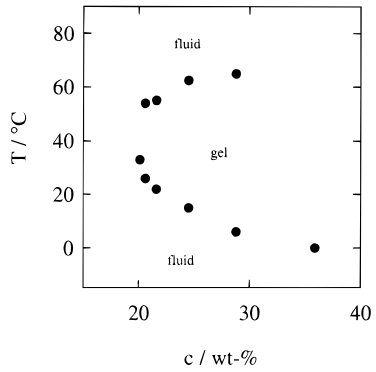

Figure 1. Phase diagram for aqueous solutions of copolymer $E_{58}B_{17}E_{58}$ showing the immobile-gel and mobile-fluid regions. The data (from ref 5) were obtained using the tube-inversion method.

Considering particularly phase behavior of the type shown in Figure 1, there is general agreement, irrespective of copolymer type (see, e.g., refs 9,14−19), that the low-temperature sol−gel boundary results from packing of micelles which are formed from molecules (unimers) in increasing proportion as the copolymer solution is heated. As the temperature is increased further, the solvent becomes progressively poorer and a number of processes occur: (i) The molecule−micelle equilibrium shifts further toward the micellar state. (ii) The average number of molecules per micelle (the association number, *N*) increases. (iii) The excluded volume of the micelle (i.e. the effective size for packing) initially increases (as *N* increases) but (as discussed below) eventually decreases as the Θ temperature of poly(oxyethylene) is approached.

[⊗] Abstract published in *Advance ACS Abstracts,* February 1, 1997.

S0024-9297(96)01520-3 CCC: $14.00

This last process provides a mechanism for the release of packing constraints and the formation of a mobile sol at high temperature.

Studies of the micellization and gelation of copolymer P85 ($E_{27}P_{39}E_{27}$) by Mortensen and Pedersen[17] and Glatter *et al.*[18] provide a second mechanism for sol formation at the high-temperature boundary, i.e. a transition from spherical to cylindrical micelles, with associated release of packing constraints. If this picture were adopted, the low- and high-temperature fluid regions in Figure 1 would be assigned, respectively, to solutions of spherical (or near spherical) and cylindrical (or near cylindrical) micelles.

An interesting feature revealed by rheological measurements on micellar solutions of certain $E_mP_nE_m$ copolymers is the formation of a complex fluid, referred to as a "soft gel".[13,19] Because of its low yield stress, it is not detected by the inverted-tube test, but it has been detected by use of a low-shear-stress rolling-ball device.[19] This soft gel has been characterized as a solution of cylindrical micelles of sufficient length to give relaxation times of the order of seconds, i.e. sufficient to give an elastic response to an oscillatory stress.[19]

In the present work we sought to minimize any compositional heterogeneity within a copolymer, since this could lead to wide distributions of micellar size, much as demonstrated for micelles of copolymers F127 (nominally $E_{106}P_{69}E_{106}$) and F88 (nominally $E_{102}P_{39}E_{102}$) by elution GPC,[20−22] and so to unwanted broadening of the sol−gel transition temperature range. Block copolymers with block length (and so composition) distributions as narrow as possible for products of anionic polymerization can be obtained by sequential copolymerization of ethylene oxide followed by 1,2-butylene oxide. This polymerization sequence avoids problems associated with the difference in reaction rates of ethylene oxide with secondary (B) oxyanions and primary (E) oxyanions.[23,24] Copolymer $E_{41}B_8$ was made in this way.

The present report concerns solutions of copolymer $E_{41}B_8$ covering the range of concentration $c = 5-70$ wt %, with particular emphasis on the rheology (oscillatory and simple shear) of solutions of $c \leq 60$ wt %. Supplementary techniques include differential scanning calorimetry and polarized-light microscopy. The study is the first of its kind for diblock copolyethers in water.

2. Copolymer $E_{41}B_8$

Copolymer $E_{41}B_8$ was prepared by sequential anionic polymerization of ethylene oxide followed by 1,2-butylene oxide (systematic name 1,2-epoxybutane) using methods similar to those described previously.[3,4] The initiator was diethylene glycol monomethyl ether partly in the form of its potassium salt. Characterization was by gel permeation chromatography and NMR spectroscopy.

The GPC system made use of three Pl-gel columns (500 Å and 2 × mixed-B). The eluent was THF at 20 °C and 1 cm^3 min^{-1} flow rate. A differential refractometer was used to detect elution of sample, and elution volumes were referenced to dodecane as internal standard. The system was calibrated with poly(oxyethylene) standards across the molar mass range 200−6000 g mol^{-1}. The GPC curve contained a single narrow peak, with molar mass at the peak $M_{pk} = 2370$ g mol^{-1} and ratio of molar mass-average to number-average molar mass $M_w/M_n = 1.04$.

NMR spectra were recorded by means of a Varian Unity 500 spectrometer operated at 125 MHz for ^{13}C spectra. Solutions were *ca.* 5 wt % copolymer in $CDCl_3$. Assignments were taken from previous work.[25] End group analysis gave $M_n = 2380$ g mol^{-1}, and compositional analysis gave 84 mol-% E (76 wt % E). Carbon intensities from end groups and junctions were equal.

Table 1. Micellization and Micellar Characteristics of Copolymer $E_{41}B_8$ in Aqueous Solution[a] (Data from Ref 26)

T/°C	cmc/(wt %)	r_h/nm	$10^{-5}M_w$/(g mol^{-1})	N_w	r_t/nm
25			0.53	22	3.8
30	0.018				
35		7.14	0.75	32	4.3
40	0.0071				
45		7.05	0.99	42	4.8
50	0.0040	7.07	1.07	45	4.9

[a] r_h and M_w determined by extrapolation of DLS and SLS data to zero concentration; r_t from the concentration dependence of the SLS data.

The micellization and micellar properties of dilute solutions of copolymer $E_{41}B_8$ were investigated by surface tension and dynamic and static light scattering measurements in related work.[26] A summary is given in Table 1, where r_h = hydrodynamic radius, M_w = mass-average molar mass, N_w = mass-average association number, and r_t = thermodynamic radius calculated from the excluded volume.

3. Experimental Methods

3.1. Preparation of Gels. Copolymer and water were weighed into a closed vessel, heated to 90 °C (2 h), and then cooled and allowed to stand for a day or so at 10 °C or lower. Samples for tube inversion were prepared *in situ*, while those for the other techniques were transferred rapidly to the appropriate holder, as described below. Minor variations of the procedure had no effect on properties.

3.2. Gel−Sol Transition Temperatures by the Tube-Inversion Method. Samples (0.5 g) were enclosed in small tubes (internal diameter *ca.* 10 mm) and observed while slowly heating (or cooling) the tube in a water bath within the range 0−85 °C. The heating/cooling rate was 0.5 deg min^{-1}. The change from a mobile to an immobile system (or vice versa) was determined by inverting the tube. The method served to define the sol−gel transition temperatures to *ca.* ±1 °C. When checked, the gels were found to be immobile in the inverted tubes over time periods of weeks.

3.3. Hot-Stage Polarized-Light Microscopy (PLM). Liquid-crystalline textures were observed by means of a Nikon Optiphot polarizing microscope equipped with a Mettler FP82HT hot-stage temperature controller. All observations were at magnification ×100. A heating rate of 1 deg min^{-1} was used over the range 0−75 °C. Evaporation of water was limited by covering the films with thin cover slips.

3.4. Rheometry. Rheological properties were determined using a Bohlin CS50 rheometer with water-bath temperature control. Couette geometry (bob, 24.5 mm diameter, 27 mm height; cup, 26.5 mm diameter, 29 mm height) was used for concentrations $c \leq 30$ wt %, with 2.5 cm^3 of sample being added to the cup in the mobile state at 5 °C. Cone-and-plate geometry (cone angle 5°, cone diameter 40 mm, gap 0.2 mm) was used for $c > 30$ wt %, with 1.5 cm^3 being transferred to the plate at room temperature. In each case 5 min was allowed for temperature equilibration before heating or cooling the sample at 1 deg min^{-1} in the range 5−90 °C. A solvent trap maintained a water-saturated atmosphere to prevent evaporation. Storage (G') and loss (G'') moduli were recorded with the instrument in oscillatory-shear mode at a frequency of 1 Hz. For all measurements the strain amplitude was low (<0.5%, linear viscoelastic region), so ensuring that G' and G'' were independent of strain. Measurements of yield stress and viscosity were made at selected temperatures with the instrument in continuous-shear mode, with at least 10 min allowed at any temperature for equilibration.

3.5. Differential Scanning Calorimetry (DSC). Measurements in the temperature range 0−100 °C were made with a Seteram Micro DSC. The samples (*ca.* 0.8 g) were sealed in steel cylinders, and distilled water was used as reference. The DSC curves of concentrated solutions of $E_{41}B_8$ showed endo-

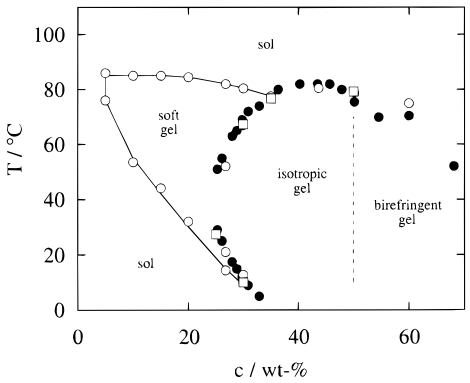

Figure 2. Phase diagram for aqueous solutions of copolymer $E_{41}B_8$. Data were obtained by (●) the tube-inversion method (heating rate = 0.5 deg min^{-1}), (○) oscillatory-shear rheometry (heating rate = 1 deg min^{-1}), and (□) differential scanning calorimetry (heating rate = 0.2 deg min^{-1}). The boundary shown by the dashed line was located by polarized-light microscopy. The notation "soft gel" and "hard gel" is that of Hvidt *et al.*[13,19]

thermic peaks on heating and corresponding exothermic peaks on cooling. At the slow heating/cooling rate of 0.2 deg min^{-1} employed, the endothermic and exothermic peaks occurred at similar temperatures, i.e. with negligible kinetic retardation. The results reported (see section 4.5) are the temperature of the minimum on heating (T_{min}) and the corresponding onset temperature (T_{onset}), the latter being defined as the intersection of the tangent at the first inflection point of the peak with the baseline. The difference between T_{min} and T_{onset} is a measure of the width of the transition.

4. Results and Discussion

4.1. Hard Gel by the Tube-Inversion Method. Results defining the phase diagram for aqueous solutions of copolymer $E_{41}B_8$ (concentration range 0−70 wt %) are shown in Figure 2. The filled circles defining the hard gel region were obtained by the tube-inversion method. Transition temperatures obtained on heating and on cooling (0.5 deg min^{-1}) agreed within 1 deg. Comparison can be made with results obtained by DSC (open squares) and rheometry (open circles). As can be seen, agreement between the three methods was excellent. Within the hard-gel region the approximate boundary between isotropic and anisotropic (birefringent) phases was determined by PLM. The results obtained by PLM, DSC, and rheometry are described and discussed below.

Systems with c > 65 wt % gave cloudy gels at low temperature and cloudy fluids at high temperature. This region of the phase diagram was not explored.

4.2. Polarized-Light Microscopy. PLM served to distinguish the isotropic (presumed cubic) phase from the anisotropic phase. The texture in the micrograph shown in Figure 3 for a 68 wt % solution is consistent with a hexagonal structure (i.e. packed cylindrical micelles). For example, it is very similar to that found previously for a 57 wt % aqueous solution of copolymer PE6400 ($E_{13}P_{30}E_{13}$).[11] The boundary drawn at 50 wt % (dashed line in Figure 2) is schematic: observations by PLM were made at intervals of 5 wt %, and textures near the boundary were indistinct. No birefringence was observed for the soft gels over the full temperature range.

4.3. Storage and Loss Modulus. Generally, storage modulus (G') and loss modulus (G'') were measured at a frequency of 1 Hz as the temperature was increased slowly from 5 to 85 °C. Transition temperatures

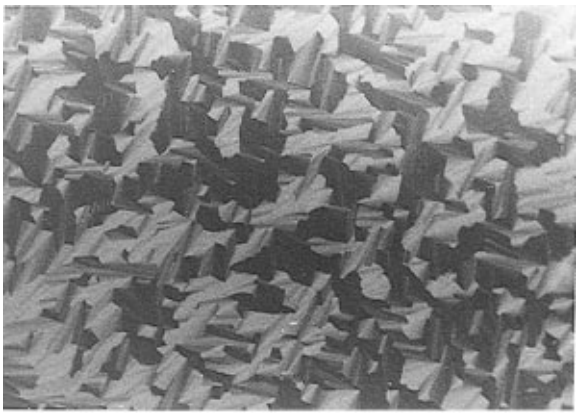

Figure 3. Polarized-light micrograph for a 68 wt % aqueous solution of copolymer $E_{41}B_8$ at 32 °C.

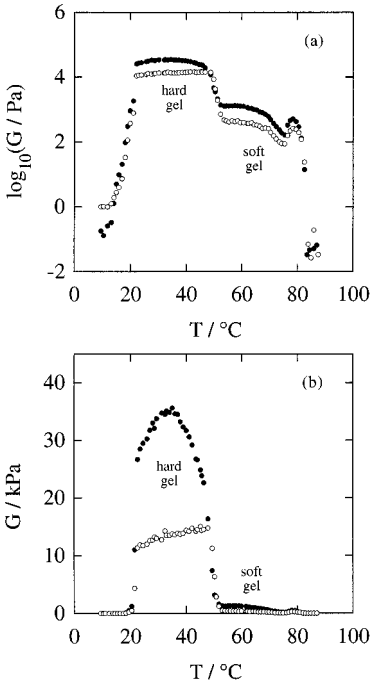

Figure 4. (a) Semilogarithmic and (b) linear plots of (●) storage modulus G' and (○) loss modulus G'' against temperature for a 27 wt % aqueous solution of copolymer $E_{41}B_8$. Heating rate = 1 deg min^{-1}. Frequency 1 Hz.

measured on cooling were approximately 2 °C lower than those measured on heating. Certain measurements were made after a temperature jump, as described below.

Measurements made at other frequencies (0.005−30 Hz) on a related copolymer (triblock $E_{21}B_{10}E_{21}$) showed that the values of G' and G'' increased with increase in frequency, in all phases: hard gel, soft gel, and sol. The effects were similar to those described by Nyström and Walderhaug[22] for copolymer $E_{78}P_{30}E_{78}$ (F68). Upper and lower hard-gel transition temperatures and upper soft-gel transition temperatures (detected by abrupt changes in the moduli, as described below) were not affected by change in frequency in the range 0.05−1 Hz. Lower soft-gel transition temperatures were sensitive to frequency, higher values being recorded at lower frequecies.

Semilogarithmic plots of G' and G'' against temperature are shown for c = 27 wt % in Figure 4a. They clearly show hard- and soft-gel regions, similar to those described for $E_{28}P_{48}E_{28}$ (Pluronic P94) copolymer solutions.[13,19] The linear plots of the moduli themselves

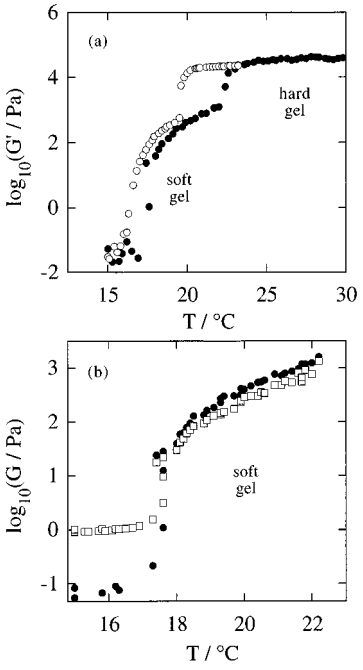

Figure 5. (a) Variation of log G' with temperature for (●) 26.5 and (○) 27.5 wt % aqueous solutions of copolymer $E_{41}B_8$. (b) Variation of (●) log G' and (□) log G'' with temperature for a 26.5 wt % aqueous solution of copolymer $E_{41}B_8$. Heating rate = 0.3 deg min^{-1}.

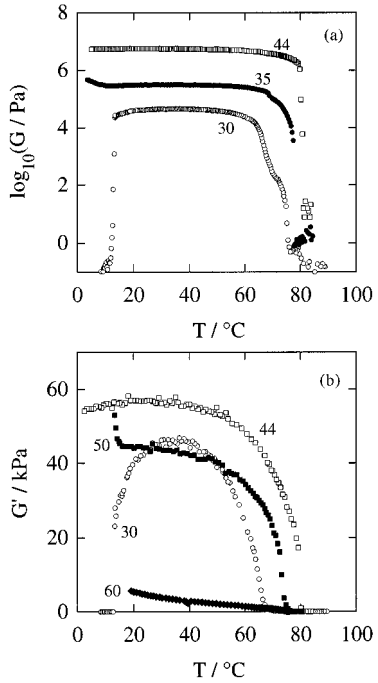

Figure 6. Plots of storage modulus G' against temperature for aqueous solutions of copolymer $E_{41}B_8$ with the concentrations (wt %) indicated. log G' is plotted in (a) and G' itself is plotted in (b). For clarity of presentation, values of log G' in (a) are displaced by +1 (35 wt %) and +2 (44 wt %) from their true values.

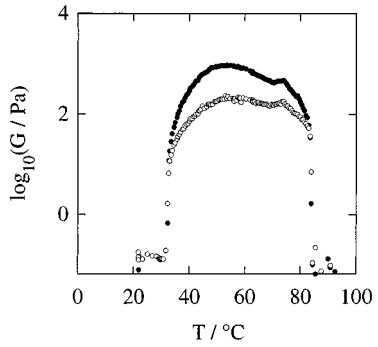

Figure 7. Semilogarithmic plots of (●) storage modulus G' and (○) loss modulus G'' against temperature for a 20 wt % aqueous solution of copolymer $E_{41}B_8$.

(Figure 4b) show more directly the large difference in modulus between the hard and soft gels and also the change in modulus through the hard-gel region. The fine structure in the soft-gel region (see Figure 4a), which is similar to that found for copolymer P94,[19] was not explored further.

The crossover point, $G' = G''$ has been proposed[28] as an indicator of the sol−gel transition. The application of this criterion to solutions of $E_mP_nE_m$ copolymers has been discussed by Hvidt *et al.*[19] and Nyström and Walderhaug.[27] For the present system it was generally possible to locate this crossover at the low-temperature boundary, but not at the other boundaries (see Figure 4a). In this work plots of the type shown in Figure 4b were used to define the transition temperatures for hard gels, since large abrupt changes in modulus were best seen in linear plots. Generally, transition temperatures were reproducible to ±2 °C. As seen in Figure 2, defining the transition temperatures for the hard gel in this way gave excellent agreement with results from the tube-inversion method. The difference between the transition temperature so defined and that defined as T when $G' = G''$ could be large, e.g. about 8 deg for the low-T boundary of the hard gel when $c = 27$ wt %.

Expansions of the semilogarithmic plots of G' against T were used to define a second region of soft gel at low temperature. Examples are shown in Figure 5. The data for $c = 26.5$ and 27.5 wt % were obtained at a slow heating rate (0.3 deg min^{-1}) for better definition of the curve. Soft-gel regions covering narrow low-temperature ranges are clearly defined in Figure 5a. The plots of G' and G' shown in Figure 5b for $c = 26.5$ wt % confirm that G'' is lower than G' over this temperature range.

The effect of increasing concentration immediately beyond 27 wt % is shown in Figure 6a (log G' *versus* T). At $c = 30$ wt % the soft-gel region is confined to a small high-temperature range (70-80 °C, compared to 50−80 °C for $c = 27$ wt %). No soft gel was detected in the high-T region for $c \geq 35$ wt % nor in the low-T region for $c \geq 30$ wt %. The plots of G' *versus* T shown in Figure 6b illustrate the lower values of G' found (across most of the temperature range) at yet higher concentrations, $c \geq 50$ wt %. The very low values of G' found for $c = 60$ wt % are attributed to the formation of a hexagonal phase, as indicated by PLM (see section 4.2). The low values found for the 50 wt % solution may be evidence of a biphasic region undefined by PLM (see section 4.2). An increase in modulus was sometimes recorded at the lowest temperatures investigated (<15 °C), but the effect was not consistent, and the cause was not determined. Examples are seen in Figure 6 ($c = 35$ and 50 wt %).

The effect of reducing the copolymer concentration below the hard-gel region is shown in Figures 7 and 8. Figure 7, a semilogarithmic plot of G' and G'' for $c = 20$ wt %, can be compared with the corresponding plot for $c = 27$ wt % (see Figure 4). Only soft gel is formed at this concentration, as evidenced by the maximum value of $G' \approx 10^3$ Pa, i.e. much the same as that of the soft gel of the $c = 27$ wt % solution and much lower (by more

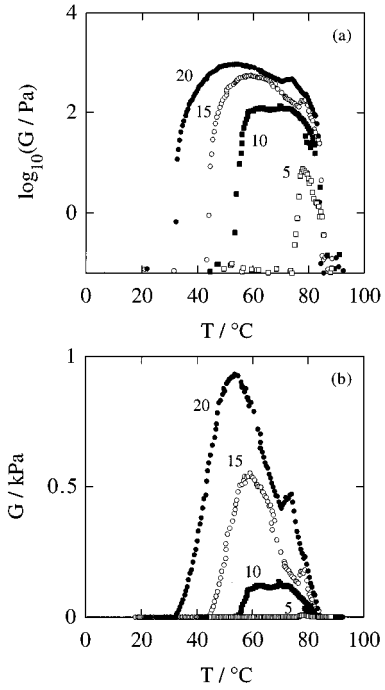

Figure 8. (a) Semilogarithmic and (b) linear plots of storage modulus G' against temperature for aqueous solutions of copolymer $E_{41}B_8$ with the concentrations (wt %) indicated.

than 1 order of magnitude) than G' of the hard gel. Nevertheless transition temperatures were readily located, even for concentrations as low as 5 wt % (see Figure 8, particularly (b)), and even though at 5 wt % the maximum value of G' was <10 Pa. Reproducibility of the low-T transition temperatures of the soft gels was ± 5 °C, which was attributed to minor changes in thermal history (see below). The raised values of G' just below the high-temperature transition (see Figure 8) mirror those found for soft gels at higher concentrations (see Figure 4).

The transition temperatures located by rheometry are plotted in Figure 2 as unfilled circles. The soft-gel region extends across a wider temperature range than that found[19] for copolymer P94. Hvidt *et al.*[19] indicated that the soft gel in that system was one containing cylindrical micelles and suggested that their hindered rotation was the origin of the elasticity. Given the present results, this may not be the explanation for the $E_{41}B_8$ gels, as discussed further in section 5. However, it is noted that the values of G' for the soft gels of $E_{41}B_8$ at a given temperature (e.g. 70 °C) plot linearly against concentration (see Figure 9), as found by Hvidt *et al.*[19] for soft gels of aqueous solutions of copolymer P94. Extrapolation to $G' = 0$ gives a concentration of *ca.* 5 wt % copolymer for first formation of the soft gel. This agrees reasonably well with the phase diagram in Figure 2, where soft gel occurs at $c \geq 5$ wt %.

It was found that the properties of the dilute soft gels ($c \leq 10$ wt %) were time dependent. The results described above were all obtained using a heating rate of 1 deg min^{-1}. A number of experiments were carried out by jumping the temperature rapidly from 20 to 75 °C, i.e. into the soft-gel region. At the lower concentrations (5 and 10 wt %) the moduli were too low to measure immediately after the T jump, and soft gel developed only after 1 h (as judged by an increase in G'). At that time the value of G' was significantly lower than that found for soft gel after slow heating to 75 °C: e.g. for the 10 wt % solution, $G' \approx 10$ Pa (measured 1 h after the T jump) compared with $G' \approx 100$ Pa (measured after slow heating). At higher concentrations (15 and 20 wt %) soft gels were present immediately after the T jump, and values of G' were essentially the same as those recorded after slow heating. A similar situation was found in the case of the L_3 (sponge) phase of copolymer PE6200 ($E_6P_{36}E_6$).[12] At high concentrations ($c \geq 20$ wt %) this very sensitive structure was formed as soon as the temperature was changed. At lower concentrations, however, it took much more than 1 h to establish the phase.

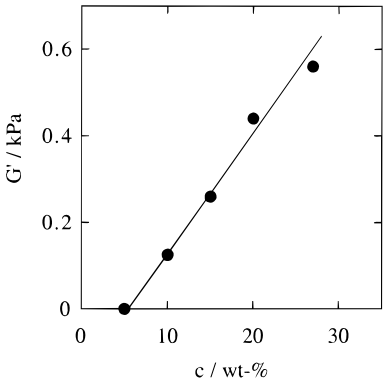

Figure 9. Storage modulus G' measured at 70 °C *versus* concentration for aqueous solutions of copolymer $E_{41}B_8$ in the soft-gel region.

4.4. Yield Stress and Viscosity. As described above, the transition temperatures found for the hard gels from plots of G' *versus* T agreed reasonably well with those found by the tube-inversion method. Considering the different physical bases of the two methods, this agreement must be ascribed mainly to the sharpness of the transitions. Since the inverted-tube method is sensitive to yield stress, this property was briefly investigated for gels formed at selected concentrations and temperatures.

Results obtained with the rheometer in continuous-shear mode are illustrated in Figure 10. The data (shear stress *versus* shear rate) are for $c = 27$ wt % and were obtained following jumps from one temperature to another. At least 10 min was allowed for equilibration following a temperature jump, at which time a selected shear stress was applied and the induced shear rate recorded until the system reached a steady state. The delay (relaxation) time employed before application of the next stress was varied in order to define conditions under which the results were insensitive to this parameter.

Plots are shown for mobile sol at 8 °C, gel at 20, 40, and 65 °C; and mobile sol at 88 °C. 20 °C is at (or just below) the soft/hard gel transition temperature, 40 °C is in the hard-gel region, and 65 °C is in the upper soft-gel region. Across the range of shear stress investigated, the two sols were Newtonian fluids, while the soft gels were complex fluids having significant yield stresses (see Table 2) followed by Newtonian flow, but with shear thickening at high shear stress for the high-T gel (65 °C). As expected, the hard gel had a large yield stress (≥1000 Pa), and the low viscosity after yield caused the rheometer to stall: the line drawn for $T =$ 40 °C in Figure 10b is based on shear rate ≥ 1000 s^{-1} at the next shear stress value (1100 Pa). The yield stresses and viscosities obtained for $c = 27$ wt % (and one other result for $c = 44$ wt % hard gel) are summarized in Table 2, together with related values of G'. The viscosities of the sols varied from *ca.* 0.1 Pa s at

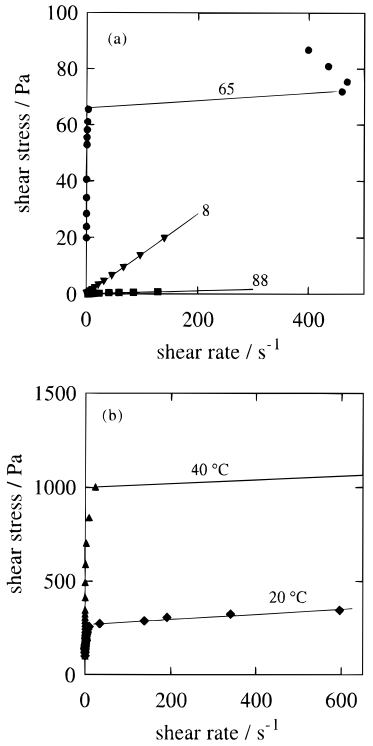

Figure 10. Shear stress *versus* shear rate for a 27 wt % aqueous solution of copolymer $E_{41}B_8$ at the temperatures indicated. Note the differences in ordinate scale between the plots for (a) the sols and the soft gel and (b) the stiffer gels.

Table 2. *T*-Jump Experiments: Yield Stress, Newtonian Viscosity (Continuous Shear), and Storage Modulus (Oscillatory Shear) for Aqueous Solutions of Copolymer $E_{41}B_8$

c/(wt %)	*T*/°C	viscosity/(Pa s)	yield stress/Pa	*G*′/Pa
44	27	*a*	*ca.* 2000	57000[b]
27	8	0.14	*a*	*a*
	20	0.11	280	1300[b]
	40	<0.1	*ca.* 1050	32000[b]
	65	*a*	65	950[b]
	88	0.007	*a*	*a*
20	75	<0.001	15	600
15	75	<0.001	4	200
10	75	*ca.* 0.0008	*a*	10
5	75	*ca.* 0.0007	*a*	*a*

[a] Too small to measure. [b] Slow-heating experiments.

low temperature to < 0.01 Pa s at high temperature; i.e. all were very mobile fluids.

Also listed in Table 2 are yield stresses and viscosities obtained from similar experiments on the soft gels formed at low concentration after a temperature jump. Consideration of the values of yield stress recorded for the various gels leads to the conclusion that the tube-inversion method (used under our conditions) will detect flow for a soft gel with a yield stress of 65 Pa, and possibly higher.

4.5. Thermodynamics of Gel Formation. DSC curves for several concentrations of $E_{41}B_8$ are plotted in Figure 11. For concentrations below 25 wt % no signals corresponding to micellization were obtained. This is in contrast to $E_mP_nE_m$ copolymers, solutions of which give a pronounced DSC signal at the critical micelle temperature (cmt).[11,12,16] Measurement (by surface tension) of cmcs at different temperatures have served to show that the critical micelle temperatures of dilute solutions of $E_{41}B_8$ are low.[26] For example, by

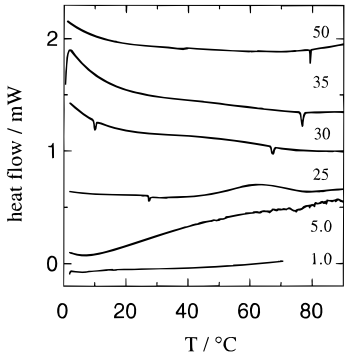

Figure 11. DSC curves (heating rate = 0.2 deg min^{-1}) for aqueous solutions of copolymer $E_{41}B_8$ with the concentrations (wt %) indicated. For clarity of presentation, curves for higher concentrations are shifted on the ordinate scale.

extrapolation of the data listed in Table 1, the concentration would need to be less than 0.1 wt % for the cmt to be above 10 °C. Moreover, the standard enthalpies of micellization of E/B copolymers are known to be significantly lower than those of E/P copolymers, e.g. by a factor of 5 or so, which has been attributed to collapse of the B block in the unassociated molecules, i.e. a form of monomolecular micelle.[3,15] In other words, the B blocks are weakly hydrated in the unassociated state, and dehydration on entering the micelle core is insignificant compared to that for P blocks.

As seen in Figure 11, the DSC curves obtained on heating solutions with $c \geq 25$ wt % show small endothermic peaks. DSC curves obtained on cooling the solutions showed corresponding exothermic transitions at similar temperatures: e.g. $c = 30$ wt %, $T_{min} = 10.0$ and 67.3 °C (heating), $T_{max} = 9.2$ and 67.3 °C (cooling).

Values of T_{min} and T_{onset} (heating) are listed in Table 3: differences ($T_{min} - T_{onset}$) in the range 0.1−0.7 are consistent with very sharp transitions. Values of T_{min} are plotted as unfilled squares in Figure 2, where they are seen to agree well with the phase boundary for hard gel (from tube inversion and rheometry). For $c \geq 30$ wt % the lower boundary is below 0 °C and outside the accessible range. Additionally, the transition from hard gel to soft gel, expected at $T \approx 50$ °C (upper boundary; see Figure 2) was not detected for $c = 25$ wt %. Transitions between sol and soft gel were never detected.

The enthalpies of the transitions measured on heating were 0.038 J (g of copolymer)$^{-1}$ (low *T*) and 0.058 J (g of copolymer)$^{-1}$ (high *T*). Given a number-average molar mass of 2380 g mol^{-1} for the copolymer, these enthalpy changes correspond to 90 J (mol of copolymer)$^{-1}$ (low-*T* boundary) and 138 J (mol of copolymer)$^{-1}$ (high-*T* boundary), with the latter corresponding to −138 J mol^{-1} for the reverse process, i.e. exothermic gelation on cooling. These enthalpies are small compared to those found by DSC for $E_mP_nE_m$ copolymers, i.e. *ca.* 1 kJ mol^{-1}.[11,12]

An alternative route to an enthalpy of gelation is to treat the association processes as a thermally reversible equilibrium, in which case

$$\text{micelles in mobile phase} \leftrightharpoons \underset{\text{(hard gel)}}{\text{associated micelles}}$$

where the mobile phase means soft gel or sol. More formally, denoting micelles as B, the equilibrium can be written

Table 3. Transition Temperatures and Enthalpies from DSC Heating Curves for Aqueous Solutions of $E_{41}B_8$[a]

	sol → gel			gel → sol		
c/(wt %)	T_{onset}/°C	T_{min}/°C	$\Delta_{gel}H$/(J g^{-1})	T_{onset}/°C	T_{min}/°C	$\Delta_{gel}H$/(J g^{-1})
25	27.0	27.4	0.011			
30	9.4	10.0	0.038	66.5	67.3	0.045
35				76.0	76.7	0.074
50				79.2	79.3	0.055

[a] Estimated uncertainty: T to ±0.05 °C; ΔH to ±0.005 J g^{-1}.

$$M\mathrm{B} \leftrightarrows \mathrm{B}_M$$

where M is a large number. Writing the equilibrium constant for 1 mol of micelles gives

$$K_{gel} = \frac{[\mathrm{B}_M]_{eq}^{1/M}}{[\mathrm{B}]_{eq}} \approx \frac{1}{[\mathrm{B}]_{eq}} \text{ (for large } M)$$

where $[\mathrm{B}]_{eq}$ is the molar concentration of micelles in equilibrium with the hard gel. For micelles of association number N,

$$[\mathrm{B}]_{eq} = [\mathrm{A}]_{eq}/N$$

where $[\mathrm{A}]_{eq}$ is the molar concentration of copolymer in the system at the hard-gel boundary at a given temperature. Consequently, the standard Gibbs energy of gelation is given by

$$\Delta_{gel}G^\circ = -RT \ln K = RT \ln([\mathrm{A}]_{eq}/N)$$

and the standard enthalpy of gelation is given by

$$\Delta_{gel}H^\circ = R\frac{\mathrm{d} \ln[\mathrm{A}]_{eq}}{\mathrm{d}(1/T)} = R\frac{\mathrm{d} \ln c_{eq}}{\mathrm{d}(1/T)} \quad (1)$$

where c_{eq} is the mass concentration (g dm^{-3}) of copolymer in the system. In this treatment the standard states are micelles in ideally dilute solution of concentration 1 mol dm^{-3} and micelles in the packed gel. This approach to the thermodynamics of gelation has been used previously.[4,14,16,29,30]

Figure 12 shows data from Figure 2 (tube-inversion method) plotted according to eq 1. Since the densities of water and the copolymer are similar, expressing the mass concentration in weight percent produces little error. The slopes of the tangents drawn at points corresponding to c = 30 wt % led to standard enthalpies of gelation of +7.9 kJ mol^{-1} (low-T boundary, 10 °C) and −9.7 kJ mol^{-1} (high-T boundary, 68 °C), where the enthalpy changes relate to moles of micelles. The quantities derived in this way relate to the overall gelation process, including contributions from changes in micellar interaction on gelation and changes in association number.

The corresponding standard enthalpies of gelation per mole of copolymer molecules are obtained by dividing by N, the association number of the micelles at the appropriate temperature. Given the data in Table 1 and noting that N plots linearly against temperature over the limited temperaure range, then $N \approx 12$ (low T) and 60 (high T), and the standard enthalpies of gelation (c = 30 wt %) are $\Delta_{gel}H^\circ \approx +600$ J (mol of copolymer)$^{-1}$ (low-T boundary) and $\Delta_{gel}H^\circ \approx -200$ J (mol of copolymer)$^{-1}$ (high-T boundary).

These standard enthalpies are larger than those measured directly by DSC. Some of this difference will originate from the temperature dependence of N, which, in DSC, contributes to the baseline rather than the peak. However, a difference between measured enthalpies from DSC and standard enthalpies from the temperature dependence of the Gibbs energy is to be expected, since they relate to different initial states. The hypothetical ideally dilute standard state allows no intermicellar interactions, whereas the real solution (c = 30 wt % copolymer) contains interacting micelles. A similar situation has been discussed for micellization of E/P copolymers[16,29,30] where it was shown that enthalpies of micellization measured by DSC were lower than the corresponding standard values, but that extrapolation of DSC enthalpies to zero copolymer concentration (i.e. zero interaction between copolymer molecules) gave comparable values.

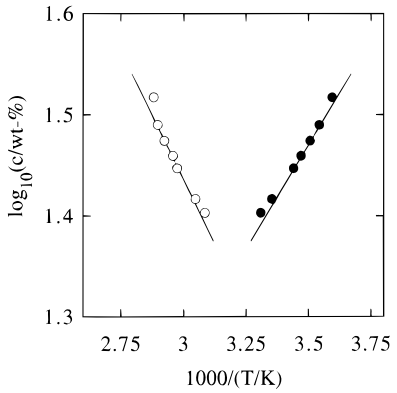

Figure 12. Plot of log c *versus* reciprocal temperature at the (●) low-T and (○) high-T hard-gel boundaries for aqueous solutions of copolymer $E_{41}B_8$. The data were obtained by the tube-inversion method.

Whichever enthalpy of gelation is considered (standard or DSC, upper or lower transition), the observed values per mole of copolymer are very small compared with those found for micellization of E/B copolymers, e.g. +78 kJ (mol of copolymer)$^{-1}$ for copolymer $E_{41}B_8$.[26] These large differences have been remarked upon previously, e.g. for E_mB_n,[14] $E_mB_nE_m$,[4] and $E_mP_nE_m$[11,16] copolymers.

5. Concluding Remarks

It is generally accepted that the cubic-phase gel can be modeled as packed hard spheres, as first shown most directly by SANS.[17,31,32] Gelation occurs when the volume fraction of spheres in the system (ϕ) reaches a critical value. This can be taken as $\phi_c \approx 0.68-0.74$ for close-packed cubic structures or as $\phi_c \approx 0.5$ for a primitive cubic structure, the latter corresponding approximately to the equilibrium condition of Hoover and Ree.[33] If an expansion factor, δ, is defined as

$$\delta = v_s/v_a$$

where v_s is the effective hard-sphere volume of the micelles in solution and v_a the "dry" volume of the micelles, then (assuming that essentially all the copolymer is in micellar form) the critical copolymer concen-

tration for gelation at a given temperature (cgc in g dm^{-3}) is given by

$$\text{cgc} = \frac{1000\phi_c\rho}{\delta} \qquad (2)$$

where ρ is the density of the copolymer in g cm^{-3}.

Parallel to the conventional treatment of polymer coils in dilute solution, the effective hard-sphere volume of a micelle (v_s) can be related to the excluded volume (u), as determined by static light scattering. In the simplest theory of dilute polymer solutions, the second virial coefficient $A_2 = N_A u/2M^2$, where N_A is Avogadro's constant and M is the molar mass. For micelles treated as hard spheres, $u = 8v_s$. The excluded volume of a polymer in solution depends sensitively on the quality of the solvent. In a poor solvent, the excluded volume is small, and in a Θ solvent it is zero. The effect reflects the balance of entropic and energetic contributions to the Gibbs energy change when polymer coils collide, and particularly the relative contributions from solvent−solvent, segment−segment, and solvent−segment interactions. In the case of micelles, the contribution of the stabilizing fringe to the excluded volume would be expected to depend on solvent quality in a parallel though not identical way. For example, the poly(oxyethylene) fringe of E_mB_n copolymer micelles would be expected to make only a small contribution to the thermodynamic volume when the solvent is a Θ solvent for poly(oxyethylene) itself. This aspect of micellar solutions (including micelles under near-Θ conditions) has been explored recently,[6] where it was shown that the critical gel concentration is satisfactorily predicted by eq 2 with $\phi_c \approx 0.7$. This is equally true in the present case. For example, use of $v_s = (4\pi/3)r_t^3$ and $v_a = M_w/N_{A\rho}$ ($\rho \approx 1.07$ g cm^{-3}) and the values of r_t and M_w in Table 1 ($T = 50$ °C) leads to $\delta = 3.05$ and so, with $\phi_c \approx 0.7$, to cgc ≈ 25 wt %, in good agreement with the hard-gel boundary at 50 °C (see Figure 2).

The observation of soft gel at the low- and high-temperature boundaries of the hard-gel region of the $E_{41}B_8$ system ($c = 27$ wt %) demands a broader interpretation of the effect than that applied to the P94 system by Hvidt *et al.*,[19] i.e. a soft gel formed from rodlike micelles. There is no evidence to support the formation of cylindrical micelles at low temperatures, and, equally, a series of transformations with increasing temperature from cylinders to spheres and back again to cylinders is unlikely. The alternative is that the soft gel is also composed of spherical micelles.

It is supposed that the soft gel comprises a dynamic network of weakly interacting spherical micelles and that the transition from sol to gel occurs when micellar aggregates with a fractal geometry reach a percolation threshold at critical micelle volume fraction ϕ_{sc} and so bridge the whole system.[34,35] The fact that the density of the water-swollen micelles is little different from water itself lends credence to this model.

Acknowledgment. We thank Mr. K. Nixon for help with characterization of the copolymers and Drs. Z. Ali-Adib and N. B. McKeown for interpretation of micrographs. Financial support came from EPSRC, Domino UK Limited (HL), DFG (SFB 213), and Fonds der chemischen Industrie (EH). The comments of our reviewer were appreciated.

References and Notes

(1) Product Brochure, B-Series Polyglycols. Butylene Oxide/Ethylene Oxide Block Copolymers, The Dow Chemical Co., Freeport, TX, 1992.
(2) Nace, V. M. *J. Am. Oil Chem. Soc.* **1996**, *73*, 1.
(3) Bedells, A. D.; Arafeh, R. M.; Yang, Z.; Attwood, D.; Heatley, F.; Padget, J. C.; Price, C.; Booth, C. *J. Chem. Soc., Faraday Trans.* **1993**, *89*, 1235.
(4) Luo, Y.-Z.; Nicholas, C. V.; Heatley, F.; Attwood, D.; Collett, J. H.; Price, C.; Booth, C.; Chu, B.; Zhou, Z.-K. *J. Chem. Soc., Faraday Trans.* **1993**, *89*, 539.
(5) Luo, Y.-Z.; Nicholas, C. V.; Attwood, D.; Collett, J. H.; Price, C.; Booth, C. *Colloid Polym. Sci.* **1992**, *270*, 1094.
(6) Deng, N.-J.; Luo, Y.-Z.; Tanodekaew, S.; Bingham, N.; Attwood, D.; Booth, C. *J. Polym. Sci., Part B: Polym. Phys.* **1995**, *33*, 1085.
(7) Schmolka, I. R. *J. Biomed. Mater. Res.* **1972**, *6*, 571. Lunsted, L. G.; Schmolka, I. R. In *Block and Graft Copolymerization*; Ceresa, R., Ed.; John Wiley and Sons: London, 1976; Vol. 2.
(8) Bahadur, P.; Panya, K. *Langmuir* **1992**, *8*, 2666.
(9) Malmsten, M.; Lindman, B. *Macromolecules* **1992**, *25*, 5440.
(10) Mortensen, K. *Europhys. Lett.* **1992**, *19*, 599.
(11) Wanka, G.; Hoffmann, H.; Ulbricht, W. *Macromolecules* **1994**, *27*, 4145.
(12) Hecht, E.; Mortensen, K.; Hoffmann, H. *Macromolecules* **1995**, *28*, 5465.
(13) Almgren, M.; Brown, W.; Hvidt, S. *Colloid Polym. Sci.* **1995**, *273*, 2.
(14) Bedells, A. D.; Arafeh, R. M.; Yang, Z.; Attwood, D.; Padget, J. C.; Price, C.; Booth, C. *J. Chem. Soc., Faraday Trans.* **1993**, *89*, 1243.
(15) Tanodekaew, S.; Deng, N.-J.; Smith, S.; Yang, Y.-W.; Attwood, D.; Booth, C. *J. Phys. Chem.* **1993**, *97*, 11847.
(16) Yu, G.-E.; Deng, Y.-L.; Dalton, S.; Wang, Q.-G.; Attwood, D.; Price, C.; Booth, C. *J. Chem. Soc., Faraday Trans.* **1992**, *88*, 2537.
(17) Mortensen, K.; Pedersen, J. S. *Macromolecules* **1993**, *26*, 805.
(18) Glatter, O.; Scherf, O.; Schillen, K.; Brown, W. *Macromolecules* **1994**, *27*, 6046.
(19) Hvidt, S.; Jorgensen, E. B.; Brown, W.; Schillen, K. *J. Phys. Chem.* **1994**, *98*, 12320.
(20) Wang, Q.-G.; Yu, G.-E.; Deng, Y.-L.; Price, C.; Booth, C. *Eur. Polym. J.* **1993**, *29*, 665.
(21) Draper, M. D.; Savage, M.; Collett, J. H.; Attwood, D.; Price, C.; Booth, C.; Wang, Q.-G. *Pharm. Res.* **1995**, *12*, 1231.
(22) Yu, G.-E.; Altinok, H.; Nixon, K.; Booth, C.; Hatton, T. A.; Alexandridis, P. *Eur. Polym. J.*, accepted.
(23) Nace, V. M.; Whitmarsh, R. H.; Edens, M. W. *J. Am. Oil Chem. Soc.* **1994**, *71*, 777.
(24) Yu, G.-E.; Yang, Y.-W.; Yang, Z.; Attwood, D.; Booth, C.; Nace, V. M. *Langmuir* **1996**, *12*, 3404.
(25) Heatley, F.; Yu, G.-E.; Sun, W.-B.; Pywell, E. J.; Mobbs, R. H.; Booth, C. *Eur. Polym. J.* **1990**, *26*, 583.
(26) Yu, G.-E.; Yang, Z.; Attwood, D.; Price, C.; Booth, C. *J. Phys. Chem.*, submitted.
(27) Nyström, B.; Walderhaug, H. *J. Phys. Chem.* **1996**, *100*, 5433.
(28) Tung, C. Y. M.; Dynes, P. J. *J. Appl. Polym. Sci.* **1982**, *27*, 569.
(29) Deng, Y.-L.; Yu, G.-E.; Price, C.; Booth, C. *J. Chem. Soc., Faraday Trans.* **1992**, *88*, 1441.
(30) Deng, Y.-L.; Price, C.; Booth, C. *Eur. Polym. J.* **1994**, *30*, 103.
(31) Wanka, G.; Hoffmann, H.; Ulbricht, W. *Colloid Polym. Sci.* **1990**, *268*, 101.
(32) Mortensen, K.; Brown, W.; Nordén, W. *Phys. Rev. Lett.* **1992**, *68*, 2340.
(33) Hoover, W. G.; Ree, F. H. *J. Chem. Phys.* **1968**, *49*, 3609.
(34) Dickenson, E.; Elvington, C.; Euston, S. R. *J. Chem. Soc., Faraday Trans. 2*, **1989**, *85*, 891.
(35) Stauffer, F.; Coniglio, A.; Adam, M. *Adv. Polym. Sci.* **1982**, *44*, 103.

MA961520A